

Continuum Coupling and Spectroscopic Properties of Nuclei

N. Michel,^{1, 2, 3} W. Nazarewicz,^{1, 2, 4} M. Płoszajczak,⁵ and J. Rotureau^{1, 2, 3}

¹ Department of Physics and Astronomy, University of Tennessee, Knoxville, Tennessee 37996

² Physics Division, Oak Ridge National Laboratory, Oak Ridge, Tennessee 37831

³Joint Institute for Heavy Ion Research, Oak Ridge National Laboratory, P.O. Box 2008, Oak Ridge, Tennessee 37831

⁴ Institute of Theoretical Physics, University of Warsaw, ul. Hoża 69, 00-681 Warsaw, Poland

⁵ Grand Accélérateur National d'Ions Lourds (GANIL),

CEA/DSM - CNRS/IN2P3, BP 55027, F-14076 Caen Cedex, France

(Dated: June 23, 2018)

The nucleus is a correlated open quantum many-body system. The presence of states that are unbound to particle emission may have significant impact on spectroscopic properties of nuclei. In the framework of the continuum shell model in the complex momentum-plane, we discuss salient effects of the continuum coupling on the spectroscopic factors, one-neutron overlap integrals, and energies of excited states in ${}^6\text{He}$ and ${}^{18}\text{O}$. We demonstrate the presence of non-perturbative threshold effects in many-body wave functions of weakly bound and unbound states.

PACS numbers: 03.65.Nk, 21.60.Cs, 21.10.Dr, 24.50.+g, 25.70.Ef

One of the main frontiers of nuclear science is the structure of short-lived, radioactive nuclei with extreme neutron-to-proton asymmetry. Such nuclei inhabit outskirts of the chart of the nuclides, close to the particle drip lines, where the nuclear binding comes to an end. In this context, the major challenge for nuclear theory is to develop theories and algorithms that would allow to understand properties of those exotic physical systems possessing new and different properties [1, 2]. To this end, a unification of structure and reaction aspects of weakly bound or unbound nuclei, based on the open quantum system (OQS) formalism, is called for.

The nuclear shell model (SM) is the cornerstone of our understanding of nuclei. In its standard realization [2, 3], SM assumes that the many-nucleon system is perfectly isolated from an external environment of scattering states and decay channels. The validity of such a closed quantum system (CQS) framework is sometimes justified by relatively high one-particle (neutron or proton) separation energies in nuclei close to the valley of beta stability. However, weakly bound or unbound nuclear states cannot be treated in a CQS formalism. A consistent description of the interplay between scattering states, resonances, and bound states in the many-body wave function requires an OQS formulation (see Refs. [4, 5] and references quoted therein). Properties of unbound states lying above the particle (or cluster) threshold directly impact the continuum structure. Coupling to the particle continuum is also important for weakly bound states, such as halos. A classic example of a threshold effect is the Thomas-Ehrman shift [6] which manifests itself in the striking asymmetry in the energy spectra between mirror nuclei. Another example is the so-called helium anomaly [7], i.e., the presence of higher one- and two-neutron emission thresholds in ${}^8\text{He}$ than in ${}^6\text{He}$.

In this work, we investigate the impact of the non-resonant continuum on spectroscopic properties of weakly bound and unbound nuclei. In particular, the one-neutron overlap integrals and energies of excited

states are studied using the SM in the complex k -plane, the so-called Gamow Shell Model (GSM) [8, 9, 10]. By explicit many-body calculations that fully account for a coupling to scattering space, we demonstrate the presence of a non-perturbative rearrangement in the wave function with a significantly low angular momentum single-particle (s.p.) component [11, 12].

GSM is the multi-configurational SM with a complex k s.p. basis given by the Berggren ensemble [13] consisting of Gamow states (poles of the s.p. S -matrix; sometimes called Siegert or resonant states) and the non-resonant continuum of scattering states. For a given partial wave, (ℓ, j) , the scattering states are distributed along the contour $L_+^{\ell j}$ in the complex momentum plane. The Berggren basis is generated by a finite-depth potential, and the many-body SM states are the linear combination of Slater determinants built from the s.p. Berggren states. The attractive feature of the GSM is that it can treat simultaneously both continuum effects and many-body correlations between nucleons due to the configuration mixing. All details of the formalism can be found in Ref. [8].

Single-nucleon overlap integrals and the associated spectroscopic factors (SFs) are basic ingredients of the theory of direct reactions (single-nucleon transfer, nucleon knockout, elastic break-up) [14, 15]. Experimentally, SFs can be deduced from measured cross sections; they are useful measures of the configuration mixing in the many-body wave function. The associated reaction-theoretical analysis often reveals model- and probe-dependence [16, 17, 18] raising concerns about the accuracy of experimental determination of SFs. In our study we discuss the uncertainty in determining SFs due to the two assumptions commonly used in the standard SM studies, namely (i) that a nucleon is transferred to/from a specific s.p. orbit (corresponding to an observed s.p. state), and (ii) that the transfer to/from the continuum of non-resonant scattering states can be disregarded.

The SF for a given reaction channel is defined as a real part of an overlap between the initial and final states [15]:

$$S^2 = \langle [\Psi_{A-1}^{J_{A-1}} \otimes u_{\ell j}]^{J_A} | \Psi_A^{J_A} \rangle^2, \quad (1)$$

where $|\Psi_{A-1}^{J_{A-1}}\rangle$ and $|\Psi_A^{J_A}\rangle$ are the wave functions of nuclei A and $A-1$, and $u_{\ell j}$ is the wave function of the transferred nucleon (normalized to unity). The radial part of $u_{\ell j}$ represents the one-nucleon radial overlap integral. Using a decomposition of the (ℓ, j) channel in the complete Berggren basis, one obtains:

$$S^2 = \mathcal{N} \left(\sum_b \langle \Psi_A^{J_A} | |a_{\ell j}^+(b)| | \Psi_{A-1}^{J_{A-1}} \rangle^2 \right), \quad (2)$$

where $a_{\ell j}^+(b)$ is a creation operator of a s.p. basis state that is either a discrete Gamow state or a scattering continuum state. The normalization constant \mathcal{N} is determined from the condition that $S^2=1$ when $|\Psi_A^{J_A}\rangle = |[\Psi_{A-1}^{J_{A-1}} \otimes u_{\ell j}]^{J_A}\rangle$. Since Eq. (2) involves summation over all discrete Gamow states and integration over all scattering states along the contour $L_+^{\ell j}$, the final result is independent of the s.p. basis assumed. This is in contrast to standard SM calculations where the model-dependence of SFs enters through the specific choice of a s.p. state $a_{n\ell j}^+$.

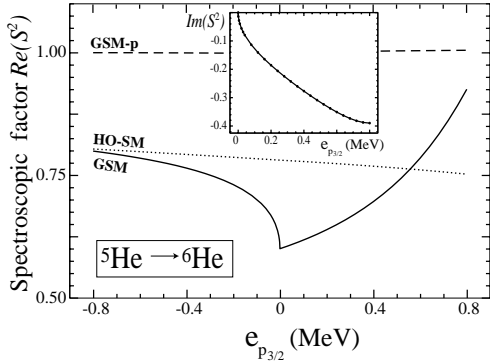


FIG. 1: The real part of the overlap $\langle^6\text{He(g.s.)}|[{}^5\text{He(g.s.)} \otimes p_{3/2}]^{0^+}\rangle^2$ in three different SM calculations as a function of the energy of the $0p_{3/2}$ resonant state. The solid line (GSM) shows the full GSM result. The dotted line (HO-SM) corresponds to the SM calculation in the oscillator basis of $0p_{3/2}, 0p_{1/2}$. The dashed line (GSM-p) shows the GSM result in the pole approximation. The imaginary part of S^2 is shown in the inset.

In the following, we shall consider the ground state (g.s.) SF of ${}^6\text{He}$ corresponding to the channel $[{}^5\text{He(g.s.)} \otimes p_{3/2}]^{0^+}$, where the single-neutron $p_{3/2}$ channel consists of the $0p_{3/2}$ resonant state and the $p_{3/2}$ non-resonant scattering states on the complex contour $L_+^{p_{3/2}}$. The

s.p. basis is generated by a Woods-Saxon (WS) potential with the “ ${}^5\text{He}$ ” parameter set [8] which reproduces the experimental energies and widths of known s.p. resonances $3/2_1^-$ and $1/2_1^-$ in ${}^5\text{He}$. The GSM Hamiltonian is a sum of the WS potential, representing the inert ${}^4\text{He}$ core, and the two-body interaction among the valence neutrons. The latter is approximated by a finite-range surface Gaussian interaction [9] with the range $\mu=1$ fm and the coupling constants depending on the total angular momentum J of the neutron pair: $V_0^{(0)} = -403$ MeV fm 3 , $V_0^{(2)} = -392$ MeV fm 3 . These constants are fitted to reproduce the g.s. binding energies of ${}^6\text{He}$ and ${}^7\text{He}$ in GSM.

In order to investigate the continuum coupling, the depth of the WS potential is varied so that the $0p_{3/2}$ s.p. state (the lowest $p_{3/2}$ pole of the S -matrix), which is also the g.s. of ${}^5\text{He}$ in our model space, changes its character from bound to unbound. The valence space for neutrons consists of the $0p_{3/2}$ resonant state, complex-momentum $p_{3/2}$ scattering continuum, and non-resonant $p_{1/2}$ scattering states along the real- k axis. We do not consider the $0p_{1/2}$ broad resonance explicitly in the basis as it plays a negligible role in the g.s. wave function of ${}^6\text{He}$ [8]. For both $L_+^{\ell j}$ -contours, the maximal value for k is $k_{\max} = 3.27$ fm $^{-1}$. The contours have been discretized with up to 60 points and the attained precision on energies and widths is better than 0.1 keV.

The calculated SF $[{}^5\text{He(g.s.)} \otimes p_{3/2}]^{0^+}$ in ${}^6\text{He}$ is shown in Fig. 1 as a function of the energy of the $0p_{3/2}$ pole. The SF strongly depends on the position of the pole: for $e_{0p_{3/2}} < 0$ it decreases with $e_{0p_{3/2}}$ while it increases for $e_{0p_{3/2}} > 0$. At the one-neutron (1n) emission threshold in ${}^5\text{He}$, $e_{0p_{3/2}}=0$, the SF exhibits a cusp. At this point, the derivative of SF becomes discontinuous, and the coupling matrix elements between the resonant $0p_{3/2}$ state and the non-resonant continuum reaches its maximum [12]. Our calculations are consistent with the early estimate of the behavior of the cross section near the threshold energy by Wigner [11]. The quickly varying component of SF below the 1n threshold in ${}^5\text{He}$ behaves as $(-e_{j\ell})^{\ell-1/2}$. Above the threshold, SF is complex; the real part behaves as $(e_{j\ell})^{\ell+1/2}$ while the imaginary part, associated with the decaying nature of ${}^5\text{He}$, behaves as $(e_{j\ell})^{\ell-1/2}$.

To assess the role of the continuum, both resonant and non-resonant, the GSM results are compared in Fig. 1 with the traditional SM approach (HO-SM) and with the GSM in the pole approximation (GSM-p). In the SM-HO variant, the harmonic oscillator (HO) basis containing $0p_{3/2}$ and $0p_{1/2}$ states with $\hbar\omega = 41A^{-1/3}$ MeV was used. The s.p. energies were taken from the GSM and their imaginary parts were ignored. The resulting SF varies little in the studied energy range and no threshold effect is seen. It is interesting to note that in the limit of an appreciable binding, the $0p_{3/2}$ wave function is fairly well localized, the importance of the continuum coupling is diminished, and the SM-HO result approaches the GSM limit. In the GSM-p variant, only the $0p_{3/2}$ and

$0p_{1/2}$ resonant states are retained in the basis, i.e., the non-resonant scattering states are ignored. Here, the g.s. of ${}^6\text{He}$ is described by an almost pure $[0p_{3/2} \otimes 0p_{3/2}]^{0^+}$ configuration and the resulting SF is close to one in the whole energy region considered. A dramatic difference between GSM and GSM-p results illustrates the impact of the non-resonant continuum.

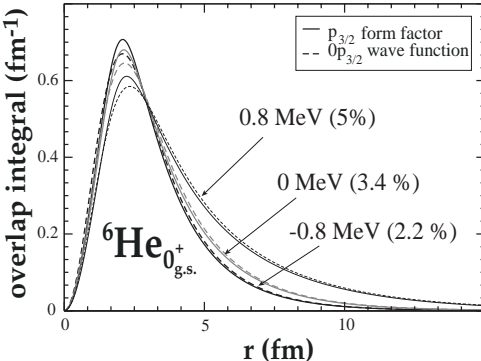


FIG. 2: Solid line: one neutron radial overlap integral for $\langle {}^6\text{He}(\text{g.s.}) | [{}^5\text{He}(\text{g.s.}) \otimes p_{3/2}]^{0^+} \rangle^2$ in GSM for three energies ($-0.8, 0, 0.8$ MeV) of the $0p_{3/2}$ resonant state. Dashed line: radial wave function of the $0p_{3/2}$ resonant state of the WS Hamiltonian adjusted to reproduce the 1n separation energy of ${}^6\text{He}$ in GSM. The relative difference between corresponding $\langle r^2 \rangle$ (in percents) is also given.

Figure 2 displays the associated 1n radial overlap integral calculated in the GSM for three energies of the $0p_{3/2}$ resonant state. With $e_{0p_{3/2}}$ increasing, the overlap becomes more diffused. For comparison, we also show the radial wave function of the $0p_{3/2}$ resonant state of the WS potential with a depth adjusted to reproduce the 1n separation energy of ${}^6\text{He}$ calculated in GSM. The agreement between s.p. wave functions and many-body overlap integrals is excellent. Asymptotically, both quantities fall down exponentially with a decay constant determined by the 1n separation energy of ${}^6\text{He}$. The effect of the non-resonant continuum is seen in a slightly better localization of GSM overlaps. (The squared radii of overlap integrals are reduced by several percent as compared to those of s.p. states.)

To investigate the dependence of SFs on the orbital angular momentum ℓ of the S -matrix pole, we show in Fig. 3 the SF for the excited 0_3^+ state of ${}^{18}\text{O}$ in the channel $[{}^{17}\text{O}(3/2_1^+) \otimes d_{3/2}]^{0^+}$. Here, the s.p. basis is generated by a WS potential with the “ ${}^{17}\text{O}$ ” parameter set [8] that reproduces experimental energies and widths of the $5/2_1^+$ and $1/2_1^+$ bound states and the $3/2_1^+$ resonance in ${}^{17}\text{O}$. As a residual interaction, we took the surface delta interaction [8] with the coupling constant $V_0 = -700$ MeV fm³, which was fitted to reproduce the g.s. binding energy of ${}^{18}\text{O}$ relative to the ${}^{16}\text{O}$ core. The valence GSM space for neutrons consists of the $0d_{5/2}$, $1s_{1/2}$, and $d_{3/2}$

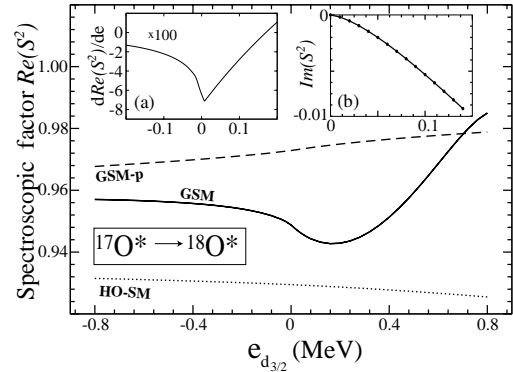


FIG. 3: Similar to Fig. 1 except for the overlap in the excited 0_3^+ state of ${}^{18}\text{O}$: $\langle {}^{18}\text{O}(0_3^+) | [{}^{17}\text{O}(3/2_1^+) \otimes d_{3/2}]^{0^+} \rangle^2$. The first derivative of the SF in the neighborhood of the $e_{0d_{3/2}} = 0$ threshold is shown in the inset (a) while the inset (b) displays the imaginary part of S^2 .

Gamow states and the non-resonant complex $d_{3/2}$ continuum. The maximal value for k on the contour $L_+^{d_{3/2}}$ is $k_{\max} = 1.5$ fm⁻¹. The contour has been discretized with 45 points and the resulting precision on energies and widths is ~ 0.1 keV.

The behavior of SF shown in Fig. 3 is similar to that of Fig. 1, except the variations are much smaller and the threshold behavior is different. Namely, the SF is continuous; it is its derivative that exhibits a cusp around the $0d_{3/2}$ threshold. Again, this is consistent with the general expectation that for $\ell=2$ $Re(S^2)$ below the 1n threshold of ${}^{17}\text{O}$ behaves as $(-e_{j\ell})^{3/2}$ while *above* the threshold $Re(S^2)$ ($Im(S^2)$) should behave as $(e_{j\ell})^{3/2}$ ($(e_{j\ell})^{5/2}$). The associated 1n $d_{3/2}$ radial overlap integrals (not displayed) are extremely close to the s.p. resonant $0d_{3/2}$ wave functions; the relative difference in square radii is around 1%.

Coupling to the non-resonant scattering continuum may change significantly energies of the many-body states close to the particle-emission threshold [5]. We now shall examine the interplay between the continuum coupling and spin-orbit splitting in ${}^5\text{He}$ and ${}^7\text{He}$ using the same GSM Hamiltonian as before. Since we are interested in the first excited $1/2^-$ state of ${}^7\text{He}$, an explicit inclusion of the $0p_{1/2}$ Gamow state is necessary. Consequently, the Berggren basis consists of the $0p_{3/2}$ and $0p_{1/2}$ resonant states and their respective complex scattering contours $L_+^{p_{3/2}}$ and $L_+^{p_{1/2}}$. We take $k_{\max} = 3.27$ fm⁻¹ for both contours, which were discretized with 27 points. The GSM eigenvalues for ${}^7\text{He}$ have been found using the Density Matrix Renormalization Group technique [19] adopted for the non-hermitian GSM problem [20].

The energy difference $\Delta E = E_{1/2_1^-} - E_{3/2_1^-}$ of the two lowest states in ${}^5\text{He}$ and ${}^7\text{He}$, calculated as a function of

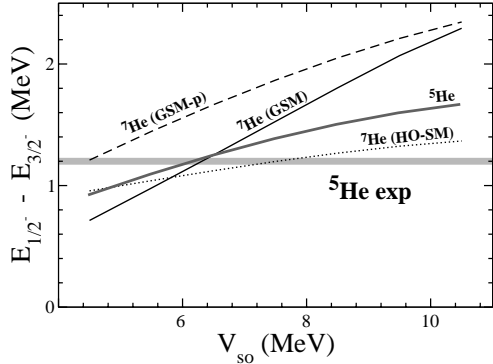


FIG. 4: The energy difference, ΔE , of $1/2^-$ and $3/2^-$ states in ^5He and ^7He as a function of the spin-orbit strength. The gray line shows ΔE in ^5He . In this case ΔE is equivalent to a s.p. spin-orbit splitting. The full GSM result for ^7He is given by the black solid line, and dotted and dashed lines mark HO-SM and GSM-p results, respectively. Experimental splitting in ^5He is indicated.

the spin-orbit term in the one-body potential, is shown in Fig. 4. In ^5He , these two states in our model space are the s.p. Gamow states $0p_{3/2}$ and $0p_{1/2}$, so that their energy difference is a spin-orbit splitting. In the absence of the residual interaction, the same splitting is obviously obtained for ^7He .

To investigate the importance of the non-resonant continuum, we have performed the complete GSM calculation in the full model space, as well as the GSM-p and HO-SM calculations. In the pole approximation, ΔE follows closely the behavior for ^5He , albeit it is slightly larger. The calculated GSM-p states in ^7He are almost the same as in the absence of the residual interaction, so the ^5He and ^7He curves differ only by a small shift due to

the residual interaction. In the HO-SM variant, the residual interaction gives rise to a configuration mixing, and ΔE in ^7He is slightly reduced as compared to the original spin-orbit splitting in ^5He . In the full GSM calculations, the coupling to the non-resonant continuum comes to the fore. The energy splitting in ^7He varies steeply with V_{so} , contrary to other curves. The difference between GSM and GSM-p results reflects different correlation energies in the $1/2^-_1$ and $3/2^-_1$ states due to a coupling to the non-resonant continuum. This means that effects of the one-body spin-orbit interaction are effectively modified by the structure of loosely bound or unbound states, so that the same interaction can lead to a different value of ΔE in neighboring nuclei.

In summary, our OQS calculations demonstrate the importance of the non-resonant continuum for the spectroscopy of weakly bound nuclei. Firstly, the GSM study shows that the behavior of SFs around the particle emission threshold exhibits a characteristic non-perturbative behavior; the predicted near-threshold reduction has, in our model, nothing to do with short-range correlations. Secondly, the continuum coupling strongly impacts the energetics of excited states (Thomas-Ehrman effect), an effect that goes well beyond the traditional CQS description. Interestingly, the effect of the non-resonant continuum on 1n overlap integrals is minor: the single-particle approximation often used in SM studies seems to work very well.

Useful discussions with the participants of the reaction part of the INT-05-3 Program “Nuclear Structure Near the Limits of Stability” at the Institute for Nuclear Theory, Seattle, are gratefully acknowledged. This work was supported by the U.S. Department of Energy under Contracts Nos. DE-FG02-96ER40963 (University of Tennessee), DE-AC05-00OR22725 with UT-Battelle, LLC (Oak Ridge National Laboratory), and DE-FG05-87ER40361 (Joint Institute for Heavy Ion Research).

[1] J. Dobaczewski and W. Nazarewicz, Phil. Trans. R. Soc. Lond. A **356**, 2007 (1998).
[2] B.A. Brown, Prog. Part. Nucl. Phys. **47**, 517 (2001).
[3] E. Caurier *et al.*, Rev. Mod. Phys. **77**, 427 (2005).
[4] C. Mahaux and H. Weidenmüller, *Shell Model Approaches to Nuclear Reactions* (North-Holland, Amsterdam, 1969).
[5] J. Okolowicz, M. Płoszajczak and I. Rotter, Phys. Rep. **374**, 271 (2003).
[6] R.G. Thomas, Phys. Rev. **81**, 148 (1951); **88**, 1109 (1952); J.B. Ehrman, Phys. Rev. **81**, 412 (1951).
[7] A.A. Oglobin and Y.E. Penionzhkevich, in *Treatise on Heavy-Ion Science, Nuclei Far From Stability*, Vol. **8** (Plenum, New York, 1989) edited by D.A. Bromley, p. 261.
[8] N. Michel *et al.*, Phys. Rev. Lett. **89**, 042502 (2002); N. Michel *et al.*, Phys. Rev. C **67**, 054311 (2003).
[9] N. Michel, W. Nazarewicz and M. Płoszajczak, Phys. Rev. C **70**, 064313 (2004).
[10] R. Id Betan *et al.*, Phys. Rev. Lett. **89**, 042501 (2002); Phys. Rev. C **67**, 014322 (2003).
[11] E.P. Wigner, Phys. Rev. **73**, 1002 (1948).
[12] J. Okolowicz and M. Płoszajczak, Int. J. Mod. Phys. E, in print; N. Michel *et al.*, Nucl. Phys. A **752**, 335c (2005); Y. Luo *et al.*, arXiv:nucl-th/0201073.
[13] T. Berggren, Nucl. Phys. A **109**, 265 (1968); T. Berggren and P. Lind, Phys. Rev. C **47**, 768 (1993).
[14] G.R. Satchler, *Direct Nuclear Reactions* (Clarendon, Oxford, 1983).
[15] M.H. Macfarlane and J.B. French, Rev. Mod. Phys. **32**, 567 (1960).
[16] Jenny Lee *et al.*, arXiv:nucl-ex/0511023.
[17] P.G. Hansen and J.A. Tostevin, Ann. Rev. Nucl. Part. Sci. **53**, 219 (2003).
[18] A. Gade *et al.*, Eur. Phys. J. A **25**, s01, 251 (2005).
[19] S.R. White, Phys. Rev. Lett. **69**, 2863 (1992); Phys. Rev.

B **48**, 10345 (1993).
[20] J. Rotureau *et al.*, to be published.